Experimental Neurology 397 (2026) 115561

Contents lists available at ScienceDirect

Experimental Neurology

journal homepage: www.elsevier.com/locate/yexnr

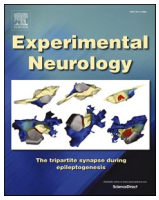

Research paper

Amelioration of transcriptional disturbances in female BACHD rats by environmental enrichment

A. Kilzheimer [a], T. Hentrich [a,b], A. Novati [a,c], H. Nguyen [c], Z. Wassouf [a], J.M. Schulze-Hentrich [a,b,*]

[a] Institute of Medical Genetics and Applied Genomics, University of Tübingen, 72076 Tübingen, Germany
[b] Department of Genetics/Epigenetics, Faculty NT, Saarland University, 66123 Saarbrücken, Germany
[c] Department of Human Genetics, Ruhr University Bochum, 44801 Bochum, Germany

ARTICLE INFO

Keywords:
Huntington's disease
Striatum
Enriched environment
Gene expression
Behaviour

ABSTRACT

Huntington's disease is a devastating neuropsychiatric hereditary illness. While progressive in nature, there is evidence suggesting the disease can be positively modified through lifestyle changes. The influence of putative protective factors can be modelled in animal models by enriched environments. As of today, there is a wide array of different implementations of environmental enrichment with little comparative information regarding their respective effects. Aiming to better understand the connection between environmental stimulation and disease progression, we examined behavioural and striatal gene expression changes in female BACHD transgenic rats exposed to either a standard environment or one of two environmental enrichment protocols differing in temporal onset. Our results show striking transgenic effects on phenotype and gene expression. Both glial and neuronal functions and cellular pathways were affected. When exposed to environmental enrichment, both protocols markedly reduced striatal dysregulation, yet some differences were observed between the two designs, thus inviting future studies to further examine the differential effects of specific paradigms. Our findings highlight the promising potential of lifestyle interventions to lighten disease burden of patients and improving their quality of life.

1. Introduction

Huntington's disease (HD) is a rare autosomal dominant neurodegenerative condition that is caused by the expansion of CAG repeats in exon 1 of the huntingtin gene (*HTT*) on chromosome 4, coding for the amino acid glutamine (Q) and thus resulting in an abnormal protein (mHTT) with excessive polyQ repeats on the amino-terminus (Bates, 2005; Zhunina et al., 2019). Due to the extended length of the polyglutamine tract, mHTT is likely to misfold and subsequently accumulate in insoluble aggregates in neurons (DiFiglia et al., 1997; Rub et al., 2016). The pathomechanism of mHTT derived cell toxicity is comprised of an array of neurotoxic effects disturbing a wide range of cellular functions and disrupting gene transcription (Cha, 2007; Kumar et al., 2014). Prominent mechanisms of neurodegeneration in HD include excitotoxicity, dopaminergic dysfunction, mitochondrial dysfunction, oxidative stress, autophagy dysregulation, and decreased trophic support (Kim et al., 2021). While HD affects several brain regions, the most prominent atrophy occurs in the basal ganglia, particularly in the striatum (Halliday et al., 1998; Waldvogel et al., 2015), where HD primarily leads to a loss of GABAergic medium spiny neurons (MSN) that make up roughly 95 % of the striatal cell composition (Ehrlich, 2012).

As a result of HD pathology, patients suffer from motor, cognitive and psychiatric deficits. Disease onset typically occurs in the fourth decade of life with a median survival of fifteen years from motor onset (Keum et al., 2016). Motor symptoms can be split into an early hyperkinetic phase with prominent choreatic movement disturbances and a later hypokinetic stage with dystonia and bradykinesia (McColgan and Tabrizi, 2018). Cognitive symptoms include slowed processing speed, impaired executive and visuospatial functions and flawed emotion recognition (Papoutsi et al., 2014). Non-cognitive psychiatric

Abbreviations: HD, Huntington's disease; mHTT, mutant Huntingtin; MSN, medium spiny neurons; WT, wildtype; TG, transgenic; BAC, bacterial artificial chromosome; EE, enriched environment; SE, standard environment; RNA-seq, RNA-sequencing; DEGs, differentially expressed genes; WGCNA, weighted gene correlation network analysis.

* Corresponding author at: Campus A2.4, 66123 Saarbrücken, Germany.
E-mail address: julia.schulze-hentrich@uni-saarland.de (J.M. Schulze-Hentrich).

https://doi.org/10.1016/j.expneurol.2025.115561
Received 9 May 2025; Received in revised form 28 October 2025; Accepted 16 November 2025
Available online 17 November 2025

disturbances include apathy, anxiety, irritability, depression, obsessive compulsive behaviour and psychosis (van Duijn et al., 2014), with non-motor symptoms usually preceding motor disturbances by years (Tabrizi et al., 2009; Tabrizi et al., 2013).

While disease burden is correlated with the extend of the individual's CAG expansion, CAG repeat length accounts for just over half of the variance in age of onset, suggesting other factors influencing HD pathology (Gusella et al., 2014). This notion is further supported by epidemiological evidence that shows environment and lifestyle bidirectionally modify disease progression (Novati et al., 2022). Physical inactivity and high caloric intake are associated with an earlier age of disease onset and more severe clinical symptoms, whereas an active lifestyle, Mediterranean diet, reduced stress and low caffeine consumption appears to be related to a less severe course of the disease (Novati et al., 2022; Marder et al., 2009; Simonin et al., 2013; Trembath et al., 2010; Trovato et al., 2022).

Animal models lend themselves to investigate such effects as they allow to draw causal inferences within environmentally and genetically standardized conditions that would otherwise not be possible to attain. Several potential HD modifying interventions have been studied, including pharmacological (Schilling et al., 2004), dietary (Kreilaus et al., 2016) and environmental (Novati et al., 2018) approaches. Regarding environmental intervention, putative protective behaviour can be induced in so-called enriched environments which have been found to have beneficial influence on the animal's phenotype by promoting physical activity, cognitive stimulation and social interaction (Mo et al., 2015). Disease modification through environmental enrichment has been shown to impact transcriptional, hormonal, neurotopological and clinical aspects of HD (van Dellen et al., 2000; Spires et al., 2004; Lazic et al., 2006; Nithianantharajah et al., 2008; Pang et al., 2009; Wood et al., 2010; Zajac et al., 2010; Wood et al., 2011; Mo et al., 2013; Benn et al., 2010; Renoir et al., 2013; Du et al., 2012; Glass et al., 2004; Gubert et al., 2022; Hockly et al., 2002; Mees et al., 2022; Zajac et al., 2018). Yet, how such environmental influences are integrated into the cellular regulatory program remains largely enigmatic. Furthermore, while there is much variation regarding the content design or augmentation of a constant enriched environment paradigm (Couly et al., 2021; Dubois et al., 2021; Mazarakis et al., 2014; Skillings et al., 2014; Steventon et al., 2015) little is known about the effect of partial environmental enrichment being present only in segments of the animals' lives (Curtin et al., 2015).

For this study, we used a transgenic animal model (BACHD rats) expressing human *mHTT* with 97 glutamine repeats that is controlled by the human *HTT* promotor and other regulatory elements, all contained in a bacterial artificial chromosome (BAC) and leading to relatively early HD-like clinical and neuropathological features (Yu-Taeger et al., 2012). We compared 6- and 12-month-old wild type (WT) and BACHD transgenic rats in either standard (SE) or enriched conditions (EE). In addition, we used two approaches for environmental enrichment that differed in their onset relative to disease progression (Fig. 1). One cohort (EE_{early}) was exposed to environmental enrichment directly after weaning, displaying the effect of an early lifelong EE, and a second cohort (EE_{late}) was initially housed in a standard environment for six months before being transferred to an EE for another 6 months. With the latter, we assessed the influence of an environmental enrichment taking place at a later age after disease progression. Thus, this study allowed us to (i) examine behavioural and molecular changes induced by mHTT expression over time, (ii) to assess the effects of environmental enrichment modulating these changes and (iii) to explore the differences between an early versus later environmental intervention.

2. Materials and methods

2.1. Animals breeding, husbandry and environmental treatments

Experiments were performed in BACHD rats and WT littermates. The BACHD rat model was generated using a BAC construct containing the whole human *HTT* locus with 20 kb upstream and 50 kb downstream flanking genomic sequences including regulatory elements and has been described before (Yu-Taeger et al., 2012). *mHTT* exon 1 carries 97 mixed CAA/CAG repeats flanked by two LoxP sites. Behavioural and weight data was collected from a cohort of 67 rats (34 BACHD and 33 WT animals) in 3 groups. Expression data was derived from a separate cohort consisting of 61 animals (31 BACHD and 30 WT rats) with three groups and two ages.

All animals were bred on a Sprague Dawley background by pairing heterozygous BACHD males with wildtype females (Charles River, Germany). As aggressive behaviour has been reported to occur between male animals housed in a long-term enriched environment (Marashi et al., 2003) only female mice were allowed to be used by the local Animal Welfare and Ethics committee of the Country Commission Tübingen, Germany (TVA HG 2/17). After genotyping, female pups

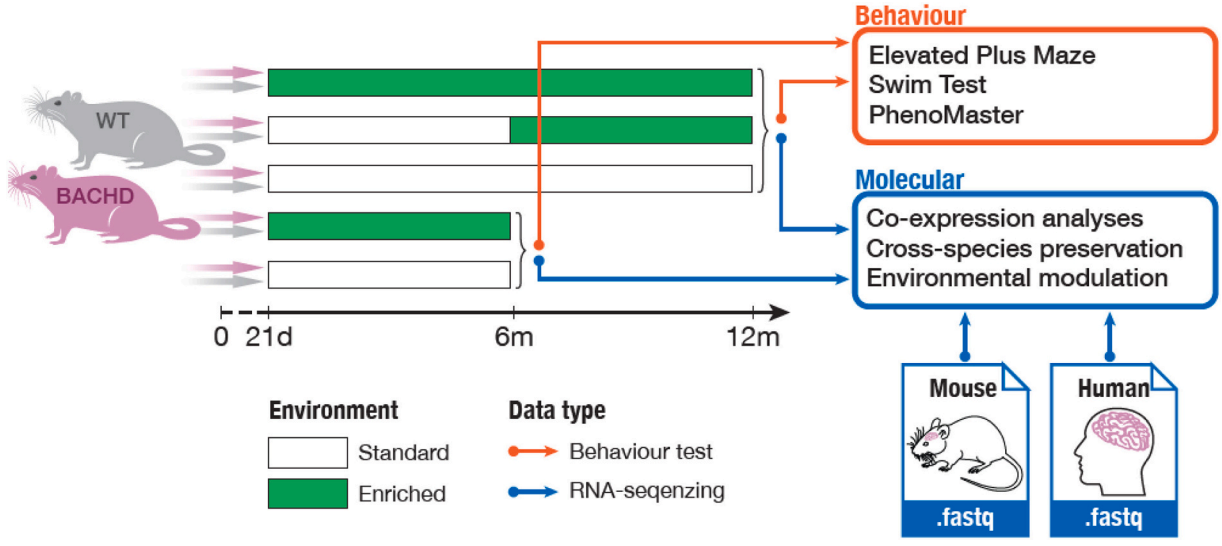

Fig. 1. Experimental design.
Groups of WT and BACHD animals (see animal numbers in Materials and Methods) were housed in a standard (SE) or enriched (EE) environment. EE was differentiated in EE_{late} and EE_{early} with animals being exposed to environmental enrichment for six or 12 months, respectively.

were randomly allocated to one of three environmental paradigms: standard environment (SE), early enriched environment (EE $_{early}$) and late enriched environment (EE $_{late}$). EE $_{late}$ cohorts were housed in standard environment for six months then transferred to an enriched environment for another 6 months. Estrous cycle was monitored in BACHD and WT rats and data were collected from rats at the same estrous cycle phase.

Examination at the selected ages of 6 and 12 months was chosen, since these time points represent critical stages in the progression of Huntington's disease-like phenotypes in this model, providing a valuable window to investigate both early manifestations and mid-stage progression of HD-related symptoms. At around 6 months, BACHD rats begin to show clear hypoactivity and early motor impairments, roughly marking the onset of behavioural symptoms that parallel aspects of HD progression; by 12 months, animals exhibit more pronounced motor deficits, though without overt neurodegeneration or striatal volume loss typical of human HD, thus allowing to assess functional changes without confounding factors related to extensive neuronal death (Yu-Taeger et al., 2012; Mantovani et al., 2016).

The environmental enrichment was achieved by maintaining novelty alongside mental and physical stimulation and social interaction. We repurposed rabbit cages (Tecniplast, 62 cm × 62 cm × 50 cm) and modified them with Plexiglas and mesh wire to spacious housing environments for the rats (Fig. S9). Two neighbouring cages were joined through doors to result in an even larger area of about 7688 cm^2. The rats were housed in groups of 12 animals in cages with running wheels, tunnels, and various toys (balls, tubes, boxes) that were rearranged once a week.

Rats in standard environment were housed in groups of four in standard type IV cages (598 × 380 × 200 mm) equipped with bedding and nesting material. All rats were housed in groups of mixed genotypes and maintained in a room with constant temperature (22 ± 1 °C), humidity (55 ± 10 %), and a regular 12 h light/dark cycle.

All procedures strictly adhered to international standards for the care and use of laboratory animals and were approved by the local Animal Welfare and Ethics committee of the Country Commission Tübingen, Germany (TVA HG 2/17). Experimenters were blinded to experimental conditions during the behavioural tests. Animals were exclusively used for this study and did not undergo experiments related to other research.

2.2. Behavioural tests

2.2.1. Running behaviour and video recordings

Two red light cameras were used to record running behaviour and usage of running wheels among WT and BACHD rats housed in EE cages. Animals were marked with non-toxic ink and videos were recorded at the beginning of the dark phase and over 3 h. WT and BACHD rats showed similar frequency in using the running wheels until the age of 6 months, afterwards the wheels were removed due to unequal usage between animals.

2.2.2. Weight monitoring

After weaning, animal weight was recorded every 2–3 weeks during the light phase.

2.2.3. Simple swim test

The test was performed over 4 days, starting with training the animals to swim to a hidden platform at one end of a rectangular water tank (150x25x40 cm). The animals were placed into the middle of the water tank facing away from the platform and trained over 3 days, two blocks of 3 trials each day. On the last day, the platform was relocated to the opposite end of the water tank (reversal trials) and time to reach the platform was recorded for each rat over two blocks of 3 trials. The test was performed during the dark phase and water temperature was kept at 28 ± 1 °C.

2.2.4. Elevated plus maze

Anxiety-like behaviour was assessed on elevated plus maze comprised of two open and two closed arms (12-cm wide and 42-cm long), connected by a 12 × 12 cm central area. The test was performed during the dark phase and the experimental room was lit with white light. Rats were placed in the centre facing an open arm and allowed to freely explore the maze over a period of 5 min. Time spent on open arms was recorded for each rat.

2.2.5. PhenoMaster

The rats' locomotor activity was tracked using the automated homecage system PhenoMaster (TSE Systems, Bad Homburg, Germany). All cages were equipped with a frame with infrared light beams for activity detection and data were recorded every 20 min over 22 h for each rat.

2.3. RNA isolation and sequencing

Animals were sacrificed by decapitation at 6 and 12 months of age. Brains were dissected and snap frozen in liquid nitrogen. Samples were then kept frozen at −80 °C.

Total RNA and DNA were simultaneously extracted from striatal samples of 6-and 12-month-old rats using the AllPrep DNA/RNA Mini Kit (Qiagen) following the manufacturer's protocol.

The polyadenylated fraction of RNA isolated from striatal tissue was used for RNA-seq. Quality was assessed with an Agilent 2100 Bioanalyzer. Samples with high RNA integrity number (RIN >8) were selected for library construction. Using the TruSeq Stranded RNA Sample Prep Kit (Illumina) and 100 ng of total RNA for each sequencing library, poly(A) selected sequencing libraries (50 bp paired-end and 75 bp single-end) were generated according to the manufacturer's instructions. All libraries were sequenced on an Illumina NextSeq and NovaSeq platform at a depth of ~15–20 million reads each. Library preparation and sequencing procedures were performed by the same individual, and a design aimed to minimize technical batch effects was chosen. Fastq files and raw counts are available through GEO (accession number pending).

2.4. Quality control and alignment

Read quality of RNA-seq data in fastq files was assessed using *FastQC* (v0.11.4) to identify sequencing cycles with low average quality, adaptor contamination, or repetitive sequences from PCR amplification. Reads were aligned using *STAR* (v2.7.0a) (Dobin et al., 2013) allowing gapped alignments to account for splicing against a custom-built genome composed of the Ensembl *Rattus norvegicus* genome v95 and the human *HTT* transgene. Alignment quality was analyzed using samtools (v1.1) (Li et al., 2009) and visually inspected in the Integrative Genome Viewer (Thorvaldsdottir et al., 2013). Normalized read counts for all genes were obtained using DESeq2 (v1.22.0) (Love et al., 2014). Transcripts covered with less than 50 reads were excluded from the analysis leaving 11,122 genes for co-expression analysis.

2.5. Weighted Gene Co-expression Network Analysis and expression analysis

All analyses were conducted with R using the packages WGCNA (Langfelder and Horvath, 2008; Langfelder and Horvath, 2012) and DESeq2 (Love et al., 2014).

We used Weighted Gene Co-expression Network Analysis (WGCNA; Zhang and Horvath, 2005) to set up the gene co-expression network. WGCNA uses the pairwise correlation of genes in the analyzed data set. As correlation method, biweight midcorrelation with maxPOutliers = 0.1 was used to minimize the influence of potential outliers. Correlations were subsequently transformed in a signed hybrid similarity matrix with positive values not being changed and negative and zero values set to

zero. The similarity matrix was raised to the power $\beta = 4$ to generate measures of network adjacency. That way, low correlations that likely reflect noise in the data are suppressed. Adjacency was then transformed into a topological overlap measure (TOM) that is informed by the adjacency of every gene pair plus the connection strength they share with neighbouring genes. TOM provides information about each gene's interconnectedness within the data set. Taking 1-TOM as an input to hierarchical clustering, modules were defined using the Dynamic Tree Cut algorithm (Langfelder and Horvath, 2008). Modules represent groups of genes that then are considered as co-expressed. Each module is summarized by an eigengene, i.e. its first principal component. Using eigengenes to identify modules affected by the transgene, eigengenes were correlated with genotype. Based on a joint Bayesian-frequentistic algorithm combining correlation Bayes Factors (BF; (Wetzels and Wagenmakers, 2012)) and significance testing, modules were checked for association with transgene status. Threshold for association was an eigengene-trait correlation of $p_{Bonferroni} \leq 0.05 \mid BF \geq 3$.

Differential expression of module genes was determined using DESeq2. Genes were considered differentially expressed with $p_{adjusted} \leq 0.10$ and a $\log 2$ *fold change* $> |0.1|$.

Preservation analyses were carried out using the WGCNA R package. Murine striatal expression data originated from (Langfelder et al., 2016). For our analysis, we decided on a subset of those animals that best matched our rat model regarding sex, age and genotype. Hence, we selected all 10-month-old female mice whose genotype was either WT or included one knock-in *mHTT* allel with CAG lengths of 140, 111, 92 or 80. Human expression data came from (Durrenberger et al., 2015; Hodges et al., 2006). Data from Durrenberger (Durrenberger et al., 2015) consisted of microarray expression data of 20 human caudate nuclei (10 Huntington patients and 10 controls). From Hodges (Hodges et al., 2006), we used microarray data from a subset of 64 human caudate nuclei (32 age- and sex-matched controls, 32 HD patients with Vonsattel Grades 0–2). Preservation meta-analysis measures were calculated by summarizing Z statistics from each data sets with Stouffer's Z, which approximately follows a normal distribution with a mean of 0 and a standard deviation of 1 (Zaykin, 2011).

2.6. Further statistical testing

Reduction in number of differentially expressed module genes in EE_{late} and EE_{early} groups was assessed via binomial tests. Non-parametric Kruskal-Wallis tests were used to analyse module genes' $\log_2$ fold change differences between the different groups since there was non-normality as well as small and unequal sample sizes in the collected data. Given non-normality, heteroscedasticity and unequal, yet relatively large sample sizes in the collected behavioural data, we resorted to Wilcox' robust statistical modelling methods best summarized in Wilcox (2017). Robust one-way (weight data) and two-way (other behavioural parameters) independent analyses of variance and robust post hoc tests were employed, both based on bootstraps of $n = 2000$ in combination with 20 % trimmed means. Where robust analyses of variance were conducted, mean differences were calculated and reported using trimmed means.

3. Results

In order to evaluate the effect of environmental enrichment in BACHD rats, we collected behavioural and striatal gene expression data for all groups at each time point, and examined mHTT-related gene expression changes and their environment- and age-dependent modulation along the experimental paradigm (Fig. 1). As outlined in the introduction, we used two approaches for environmental enrichment that differed in their onset relative to disease progression (Fig. 1). One cohort (EE_{early}) was exposed to environmental enrichment immediately after weaning, representing the effects of early and continuous EE exposure. The second cohort (EE_{late}) was first maintained in a standard environment for six months before being transferred to an EE for another six months. In the latter group, we examined the impact of environmental enrichment introduced at a later stage, following disease progression. Two distinct groups of animals were used for behavioural and molecular analyses.

3.1. mHTT induced progressive behavioural deficits in transgenic animals

First, we assessed the animals' phenotype by a battery of tests consisting of weight monitoring, Simple Swim Test (SST) for cognitive abilities, Elevated Plus Maze (EPM) for anxiety-related behaviour, and PhenoMaster (TSE Systems) for locomotor activity. A marked effect of the transgene was observed on both 6- and 12-month-old rats' phenotype across all measured domains with strong deterioration in the older cohort (Fig. 2).

In contrast to previous reports in male BACHD rats, female BACHD rats displayed a greater weight gain than WT in both environmental conditions ($F_{bootstrapped} = 32.6$, $p < .001$, post hoc comparisons $\widehat{\psi} < -51.5$, $ps_{adj} < 0.001$, $|\Delta_{robust}| > 51.9$ g, $\xi > 0.69$) (Fig. S1). While this finding stands in contrast to the initial characterization of the BACHD rats (Yu-Taeger et al., 2012), who reported no differences in weight gain in male BACHD transgenic rats, a similar effect was observed in both male and female BACHD mice (Menalled et al., 2009).

Next, SST was used to assess the animals' cognitive performance. We found that BACHD rats were slower in finding the relocated platform than WT animals in both age cohorts, hinting at reduced cognitive adaptability in BACHD animals. Six-month-old transgenic rats performed significantly worse than the WT in reverse-trial testing irrespective of environment ($\omega^2 = 0.04$, $p < .05$ with main effect of environment and interaction term being not significant, ps > 0.13). On average, WT animals reached the platform about 0.9 s faster than BACHD rats ($\widehat{\psi} = -1.96$, $p_{adj} < 0.05$, $|\Delta_{robust}| = 0.9$ s, $\xi = 0.39$) (Fig. S2 A). The 12-month-old cohort showed an even stronger main effect of genotype ($\omega^2 = 0.17$, $p < .001$) (Fig. 2A), with BACHD rats being significantly slower in reaching the platform than the WT cohorts ($\widehat{\psi} = -8.5$, $p_{adj} < 0.001$, $|\Delta_{robust}| = 3.0$ s, $\xi = 0.60$). The type of environment did not seem to affect test performance, neither did it seem to modulate the genotype effect as interactor (ps > 0.60). In combination, these results show an early and progressive mHTT-induced phenotype. This observation was different during the acquisition training of the SST. While younger animals displayed no significant differences (ps > 0.66) (Fig. S2B), the environment significantly influenced learning in the older animals ($\omega^2 = 0.09$, $p < .01$). Here, EE_{late} animals displayed greater improvement than the EE_{early} cohort ($\widehat{\psi} = -3.0$, $p_{adj} < 0.01$, $|\Delta_{robust}| = 0.57$ s, $\xi = 0.12$) (Fig. S2C). Genotype both as main effect and as co-interactor did not significantly influence learning curves (ps > 0.05).

Anxiety-like behaviour on the EPM was similar among the 6-month-old cohorts (ps > 0.11) (Fig. S2D). Yet, older BACHD rats displayed stronger anxiety-related reactions as we observed a genotype effect in 12-month-old animals ($\omega^2 = 0.05$, $p < .01$). Specifically, transgenic animals spent less time in the maze's open arms ($\widehat{\psi} = 74.8$, $p_{adj} < 0.01$, $|\Delta_{robust}| = 27.3$ s, $\xi = 0.38$) than WT animals with no influence of the environment on this behaviour (ps > 0.08) (Fig. S2E).

Lastly, PhenoMaster (PM) data indicated progressive reduction of locomotor activity in transgenic animals. Looking at ambulatory activity during dark phase, we found a significant main effect of genotype in 6-month-old rats ($\omega^2 = 0.28$, $p < .001$) (Fig. S2F). The transgenic rats were less active than WT ($\widehat{\psi} = 1188.9$, $p_{adj} < 0.001$, $|\Delta_{robust}| = 622$ cm, $\xi = 0.87$). In the 12-month-old cohorts, the effect of genotype on activity was modulated by environment ($\omega^2 = 0.05$, $p < .05$, Fig. 2B). Specifically, transgene-induced differences were smaller in EE_{late} compared to SE ($\widehat{\psi} = 227.6$, $p_{adj} < 0.05$) or EE_{early} ($\widehat{\psi} = -188.9$, $p_{adj} < 0.01$). Meanwhile, there was no significant differences between SE and EE_{early} ($\widehat{\psi} = 38.7$, $p_{adj} = 0.36$). In terms of effect sizes, we saw a strong genotype effect in each environmental condition with a significantly smaller effect

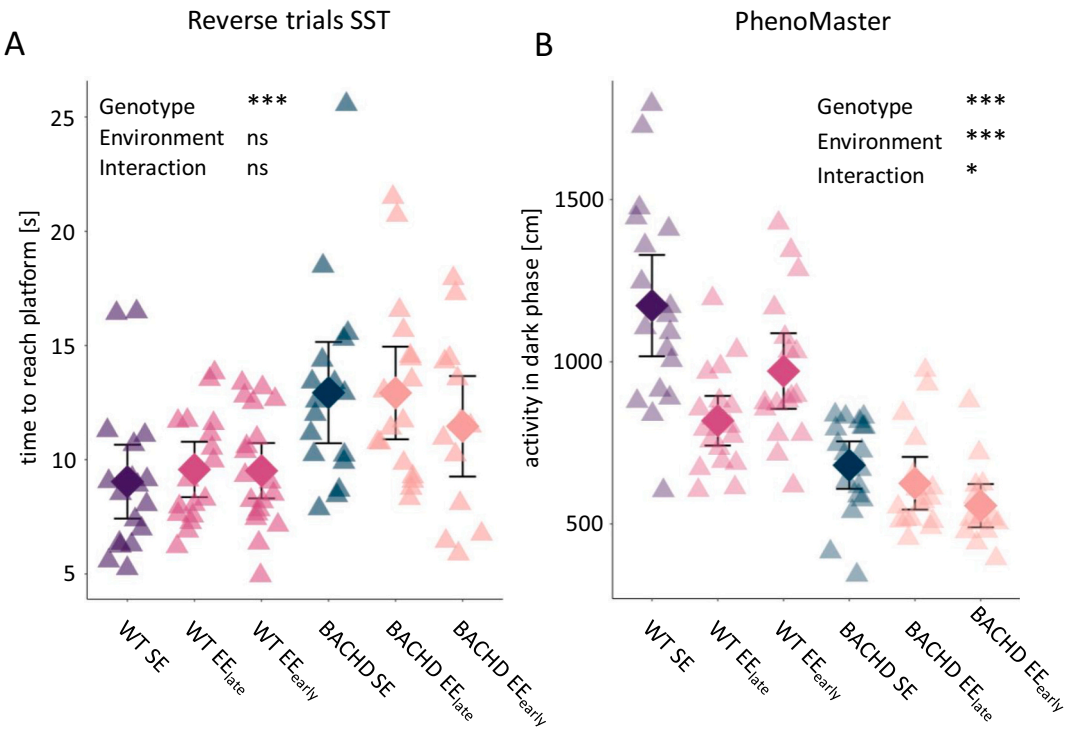

Fig. 2. Behavioural deficits in transgenic animals.
Behavioural analyses of 12-month-old animals. Significance levels of robust analyses of variance were as follows: *0.05, **0.01, ***0.001; error bars indicate 95 % confidence intervals for the mean.
(A) Reverse trial of the simple swim test. N values for each group were 19 (WT EE_{early}), 18 (WT SE), 17 (WT EE_{late}, BACHD SE, (BACHD EE_{late}) and 14 (BACHD EE_{early}), respectively.
(B) Activity during the dark phase measured via PhenoMaster. N values for each group were 18 (WT SE, WT EE_{late}, BACHD SE), 17 (WT EE_{early}, BACHD EE_{late}) and 15 (BACHD EE_{early}), respectively.

in EE_{late} ($|\Delta_{robust}|$ = 217 cm, ξ = 0.75) than in SE ($|\Delta_{robust}|$ = 445 cm, ξ = 0.97) or EE_{early} ($|\Delta_{robust}|$ = 406 cm, ξ = 0.83). Notably, the effect of environment was rather due to a decrease of activity in WT animals.

Taken together, behavioural analyses showed a strong, transgene-induced effects on cognitive, locomotor, and anxiety-related behaviour. We found evidence for an age-dependent worsening of cognitive performance and anxiety-related behaviour in transgenic rats, while locomotor functions were equally affected in both age cohorts. Moving forward, we next investigated transcriptional correlates of these effects by examining differential gene (co)expression networks.

3.2. *Network analysis revealed mHTT-dependent co-expression modules with strong preservation across environments and species*

Examining potential transgenic dysregulation on gene expression levels, a coexpression analysis was conducted (see Fig. 3). Aiming to initially infer the isolated effect of mHTT and subsequently examining a possible environmental and age-related modification of that effect, SE animals were used to set up the network and define modules that were dysregulated by mHTT overexpression. The weighted gene co-expression network analysis (WGCNA) identified 98 modules with a minimum and maximum number of module genes of 36 and 853, respectively. The complete network consisted of 11,159 genes (Fig. 3A). Module eigengenes served as summary expression profiles to correlate each module with mHTT expression. Using a joint Bayesian-frequentist approach, we identified five modules with significant mHTT association (i.e. $p_{Bonferroni} \leq 0.05$ with a *Bayes Factor* ≥ 3, Fig. 3B). All eigengenes were negatively correlated with mHTT, indicating a relative down-regulation of the module genes in transgenic animals. Correlation coefficients of the modules ranged from −0.78 to −0.71. Because of their high intramodular connectivity, hub genes based on their module membership (i.e. the correlation with the module eigengene) were identified in order to gain insight into these modules' general biological focus (Fig. S3). Hub genes in module Cyan showed enrichment for glia-focused pathways related to myelination processes and oligodendrocytic differentiation, while hub genes in module Purple were focused around catalytic activity. Hub genes of the remaining three modules (Brown2, Mediumpurple2 and Palevioletred3) showed no clear functional enrichment, indicating that their gene functionality may be too diverse for their relatively small module size to allow for meaningful functional enrichment analyses. Thus, the network analysis provided a reduction of high-dimensional transcriptional data to a relatively small number of gene co-expression clusters alongside distinct module responses to mHTT expression in transgenic rats. In addition, this analysis provided an increased sensitivity for finding differential expression patterns by mitigating statistical issues arising from multiple testing.

To further validate the identified mHTT-related modules and gain confidence that modules actually reflect robust biological functions, we carried out preservation analyses to check whether the striatal co-expression pattern found in SE animals could be validated in the remaining experimental conditions with different environment and age (Fig. 3C). We found that out of the five identified mHTT-related modules, three were sufficiently preserved in all other experimental groups (with a summary preservation Z score of at least 2), while the remaining two modules failed to meet this criterion in at least one experimental condition. Combining the single preservation summaries of the three modules into *Stouffer's Z*, a single meta-analysis statistic, showed the strongest overall preservation for modules Cyan and Purple ($Z_{Stouffer}$ = 26 and 25.5, respectively), followed by module Palevioletred3 ($Z_{Stouffer}$ = 14). Next, we investigated whether these modules were also preserved in HD mouse models and human HD patient data. We found that modules Cyan, Palevioletred3 and Purple were preserved in 10-month-old

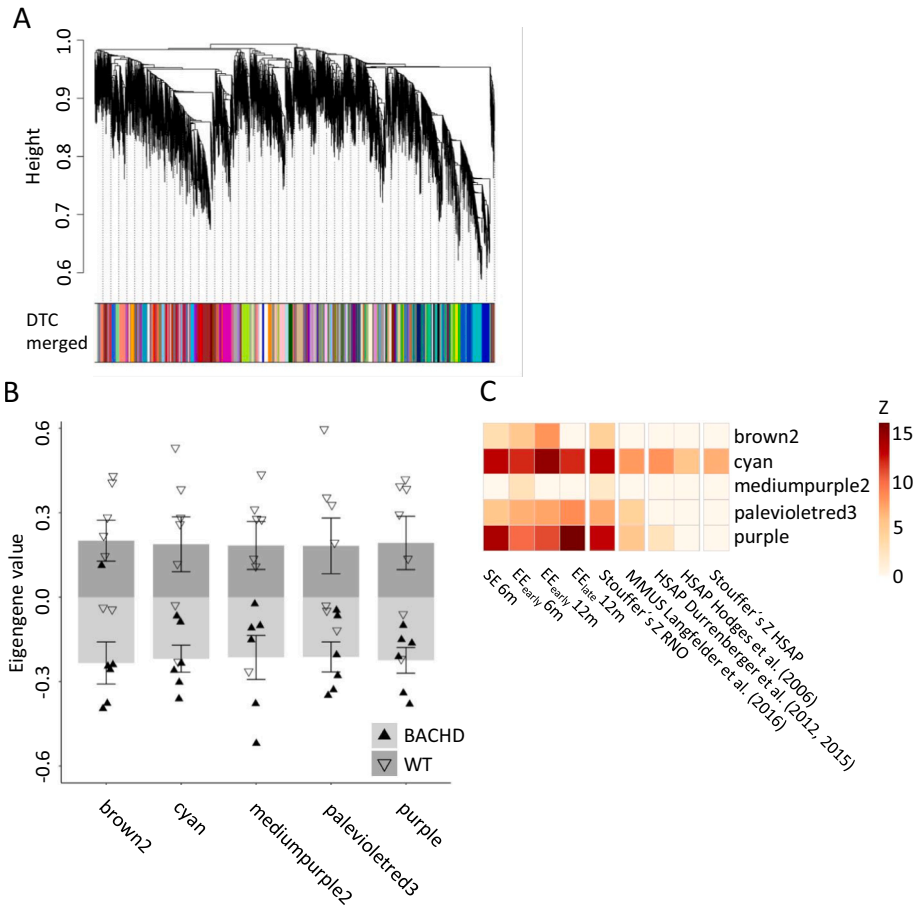

Fig. 3. Co-expression modules with strong preservation across environments and species.
(A) Dendrogram of hierarchical clustering of genes in co-expression modules in 12-month-old SE WT ($n = 7$) and BACHD ($n = 6$) animals. Each vertical line corresponds to a gene with branches representing modules of co-expression. The bar below represents the colour-coded modules that resulted from applying the DTC algorithm and merging highly correlated modules as measured by the correlation of their eigengenes ($r \geq 0.9$).
(B) Module eigengene expression in WT and BACHD animals for eigengenes significantly correlated with genotype ($p \leq .05|\text{BF} > 3$).
(C) Preservation analysis of selected modules in murine and human data sets. The modules Cyan and Purple show the strongest preservation across all data sets. (For interpretation of the references to colour in this figure legend, the reader is referred to the web version of this article.)

female mice carrying a *Htt* allele with knock-in of human *mHTT* with a CAG length between 20 and 140 (Langfelder et al., 2016). In human gene expression data sets (Durrenberger et al., 2015; Hodges et al., 2006), modules Cyan and Purple showed sufficient degree of preservation. Given the overall preservation in rodent and human expression data, these two modules were selected for further investigation.

Module Cyan contained 162 genes with an eigengene-genotype correlation of $r = -0.73$ ($BF = 10.98$, $p_{Bonferroni} = 0.028$), indicating a lower module expression in transgenic animals. Of these module genes, 84 were differentially expressed genes (DEGs) between the transgenic and WT groups (i.e., $\log_2$ fold change $\geq|0.1|$ with $p_{FDR} \leq 0.1$). Module Purple was comprised of 224 co-expressed genes with an eigengene-genotype correlation of $r = -0.71$ ($BF = 8.67$, $p_{Bonferroni} = 0.037$) and 65 DEGs, also suggesting a relative downregulation of the module in transgenic animals. Having identified and validated these co-expression modules driven by mHTT expression, we next examined their association with biological functions within the cells.

3.3. *mHTT-dependent down-regulation of module genes showed dysregulation in myelination pathways and synaptic function*

To gain an understanding of the biological relevance underlying the differential expression in mHTT-related modules, we performed functional enrichment analyses (Fig. 4A, B). Module Cyan DEGs were connected to glial functions, especially to processes related to axon ensheathment. In analogy to the module eigengene, Cyan DEGs showed a mHTT-induced reduction, indicating impaired striatal myelination processes (Fig. 4C). Among those genes are potential hallmark genes such as Myelin Associated Glycoprotein (*Mag*) and Myelin Basic Protein (*Mbp*, Fig. 5A, B). MAG is needed for the maintenance of myelinated axons as well as oligodendrocytic differentiation and (Quarles, 2007), while MBP is the second most abundant protein in myelin sheaths of the central nervous system (Boggs, 2006). MBP is vital for myelin membrane stacking and an aetiological key structure for demyelinating diseases such as multiple sclerosis (Raasakka et al., 2017).

Differential expression in module Purple also displayed downregulation in transgenic animals (Fig. 4D). DEGs were connected to synaptic functions with candidate genes including Alpha B crystallin (*Cryab*) and Dynamin 2 (*Dnm2*, Fig. 5C, D). CRYAB is a heat shock protein that serves as an autophagy inhibitor in astrocytes. Elevated levels of CRYAB are implicated in a range of protein-aggregation related neurodegenerative diseases (Lu et al., 2019). DNM2 belongs to the dynamin family mediating membrane fission. DNM2 is ubiquitously expressed and plays an important role in endocytosis and organelle division or fusion and is discussed as an aetiological cofactor of a variety of neuromuscular diseases (Zhao et al., 2018).

Having characterized differential module expression induced by mHTT in 12-month-old animals potentially underlying the observed phenotypic changes, we next conducted a comparative analysis of the 6- and 12-month-old cohorts.

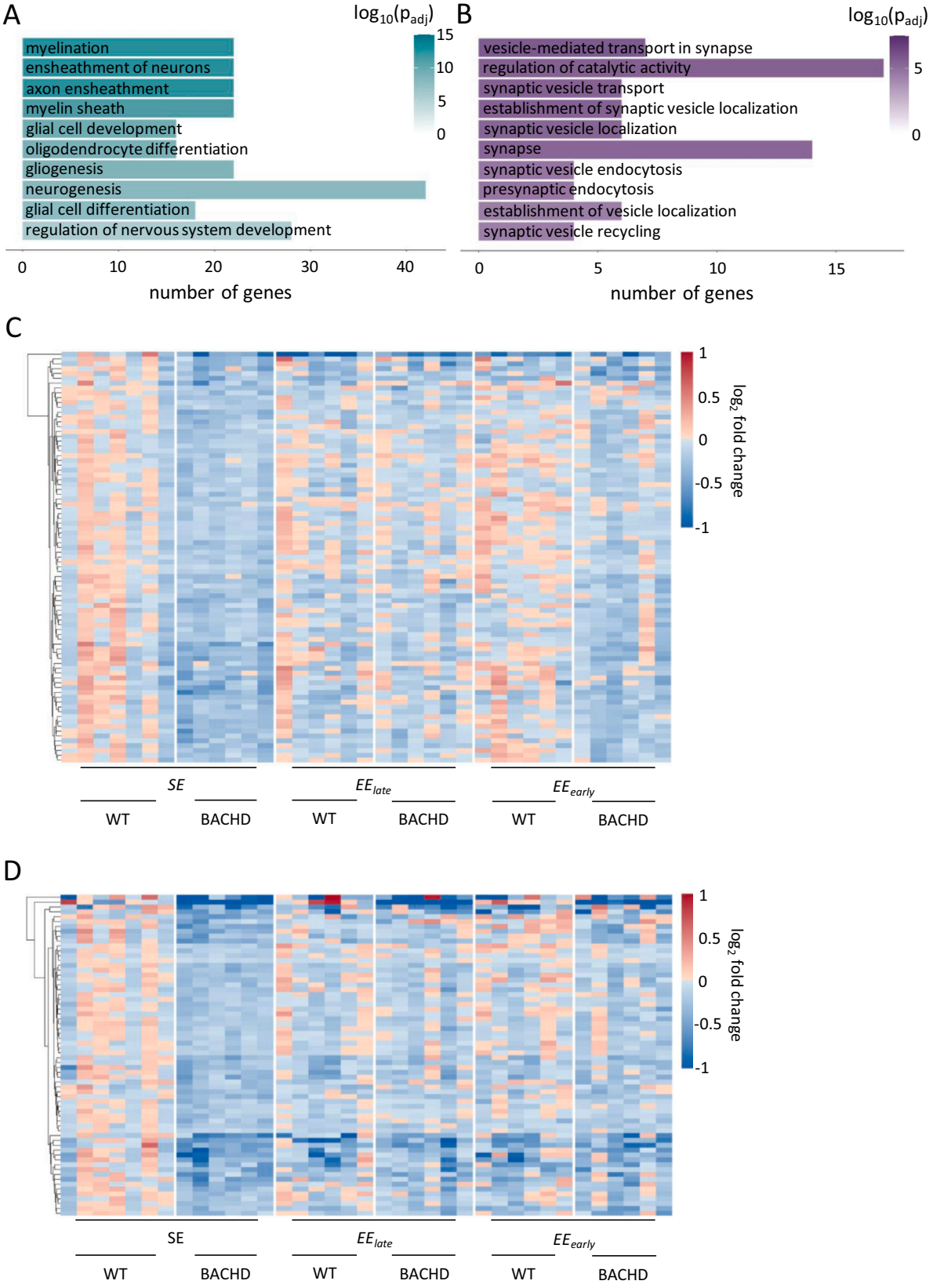

Fig. 4. Module genes showed dysregulation in myelination pathways and synaptic function.
Top 10 Gene ontology (GO)-terms identified in differentially expressed genes of module Cyan **(A)** and Purple **(B)** using g:Profiler (FDR $\leq$ 0.1).
Heatmaps show $\log_2$ fold expression changes of differentially expressed genes in module Cyan **(C)** and Purple **(D)** identified in 12-month-old SE rats across all three conditions (expression changes relative to mean of WT SE animals). (For interpretation of the references to colour in this figure legend, the reader is referred to the web version of this article.)

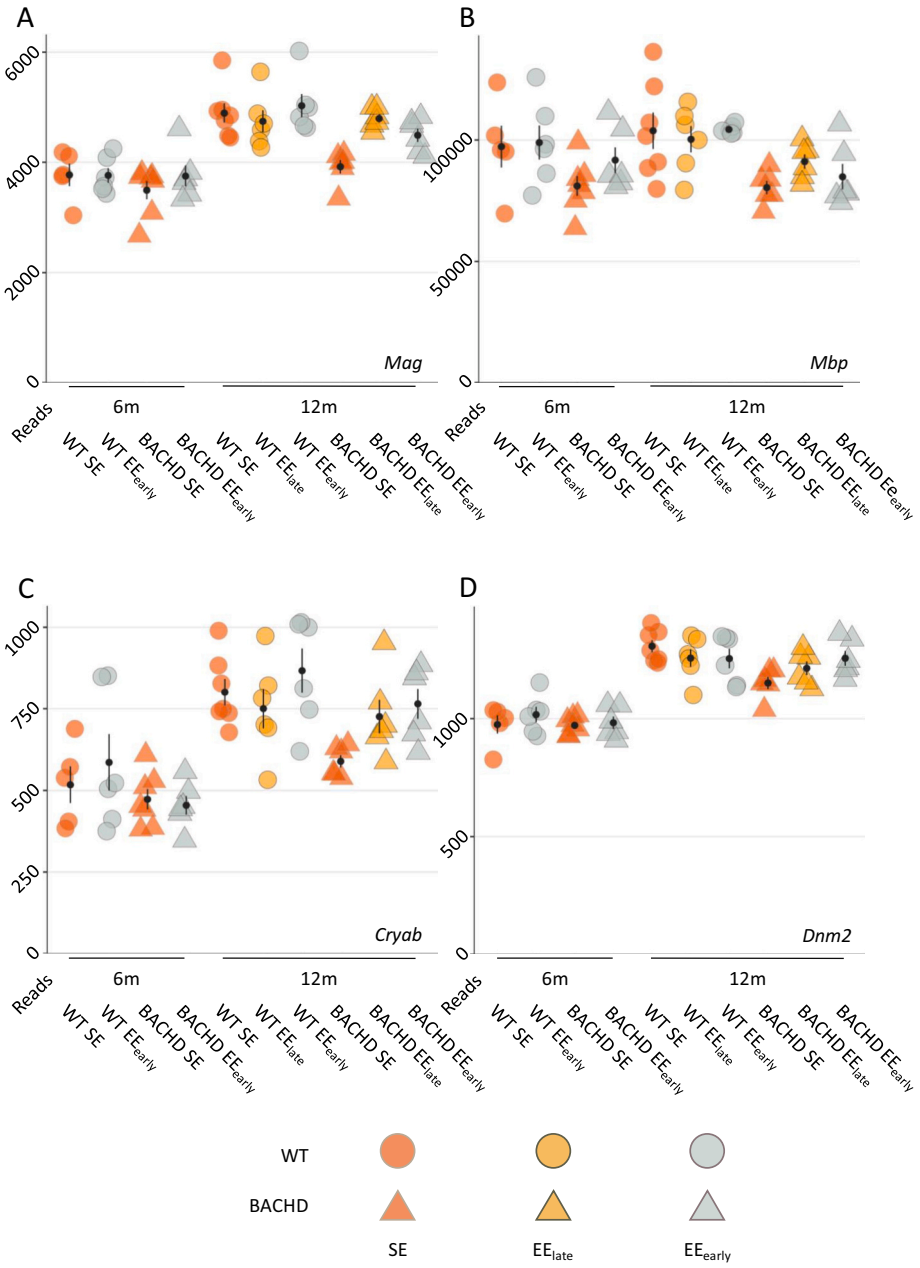

Fig. 5. RNA-seq results of selected genes partially altered by mHTT overexpression and environmental influences.
Plots show expression levels in normalized reads as individual data points with mean ± SEM. Genes in **(A)** and **(B)** are DEGs in module Cyan, whereas genes in **(C)** and **(D)** are DEGs in module Purple. N values for each group of the 6-month-old cohort were 5 (WT SE), 6 (WT EE), 7 (BACHD SE) and 6 (BACHD EE), respectively. For the 12-month-old cohort, n values were 7 (WT SE), 6 (WT EE$_{early}$), 6 (WT EE$_{late}$), 6 (BACHD SE), 6 (BACHD EE$_{early}$), 6 (BACHD EE$_{late}$), respectively. (For interpretation of the references to colour in this figure legend, the reader is referred to the web version of this article.)

3.4. Age-related transcriptional dysregulation in transgenic animals

Differential expression of module genes in 6-month data revealed very limited changes with module Cyan showing no DEGs in any of the conducted comparisons and module Purple having very few DEGs with the highest count in the comparison of SE and EE$_{early}$ BACHD animals (Fig. S4). Comparing data of both age groups, pseudo-trajectories were constructed tying genotype- and environment-matched animals across both ages.

Comparing 6- and 12-month data, the expression in both modules was strongly influenced by the animals' age (Fig. S5–7). In module Cyan, between 85 and 99 genes were differentially expressed between the time points, depending on the examined pseudo-trajectory. Age-dependent differential expression in module Purple ranged from 133 to 155 genes. In both modules, the particular genes were largely shared between all pseudo-trajectories. These shared DEGs displayed a tendency for stronger upregulation in WT animals, while their expression changes in BACHD rats were less pronounced. In addition, age-related DEGs in WT animals were upregulated in older rats, while these genes remained unchanged in BACHD.

In summary, comparable age-related trajectories in module expression were observed between both genotypes with BACHD animals partially failing to reach or maintain expression levels displayed by their WT counterparts.

3.5. Environmental enrichment prevented transcriptional disturbances across co-expressed gene modules

The widespread transcriptional disturbances associated with mHTT in the selected transgene-dependent modules with lower expression in transgenic animals were normalized in both EE conditions. Fig. 4C and D show that the downregulation of identified DEGs in the 12-month-old SE cohort was at least partially ameliorated in EE_{early} and EE_{late} conditions. In Module Cyan, DEGs were associated with pathways related to myelination processes and glial cell development. Compared to 84 DEGs in SE conditions, the number of DEGs in the module was one (EE_{early}, $p_{Bonferroni} < 0.001$, $OR = 0.006$) and zero (EE_{late}, $p_{Bonferroni} < 0.001$, $OR = 0$) in each respective EE condition. The one gene differentially expressed between the genotypes in EEearly conditions, *Chd7*, was also a DEG in SE conditions. Module Purple DEGs in SE conditions were associate with pathways pertaining to synaptic vesicle regulation. Compared to 65 DEGs in SE, differential expression in that module was drastically lower in EE conditions with three (*Syt10*, *RGD1310587*, *Tril*) in EE_{early} ($p_{Bonferroni} < 0.001$, $OR = 0.033$) and one (*Syt10*) DEG in EE_{late} ($p_{Bonferroni} < 0.001$, $OR = 0.011$), respectively, with *Syt10* being also differentially expressed in SE conditions. Outcome measures of both modules within the same environment showed similar results (Fig. S8).

This remarkable effect on the number of differentially expressed genes was paralleled by quantitative assimilation of expression ratios between the environments (Fig. 6). We found that environmental conditions significantly influenced $\log_2$ fold gene expression changes in both modules ($H_{Cyan}(2) = 107.01$, $p < .001$, and $H_{Purple}(2) = 45.943$, $p < .001$). Comparisons of mean ranks between groups showed that in both modules, median LFC was significantly higher in SE than in EE_{early} ($difference_{Cyan} = 64.5$, $difference_{Purple} = 51.4$) as well as in EE_{late} ($difference_{Cyan} = 116.1$, $difference_{Purple} = 63.1$). Interestingly, expression differences between the genotypes were even lower in the EE_{late} than in EE_{early} group for module Cyan genes ($difference = 51.6$), while there was no significant difference between the EE conditions in module Purple

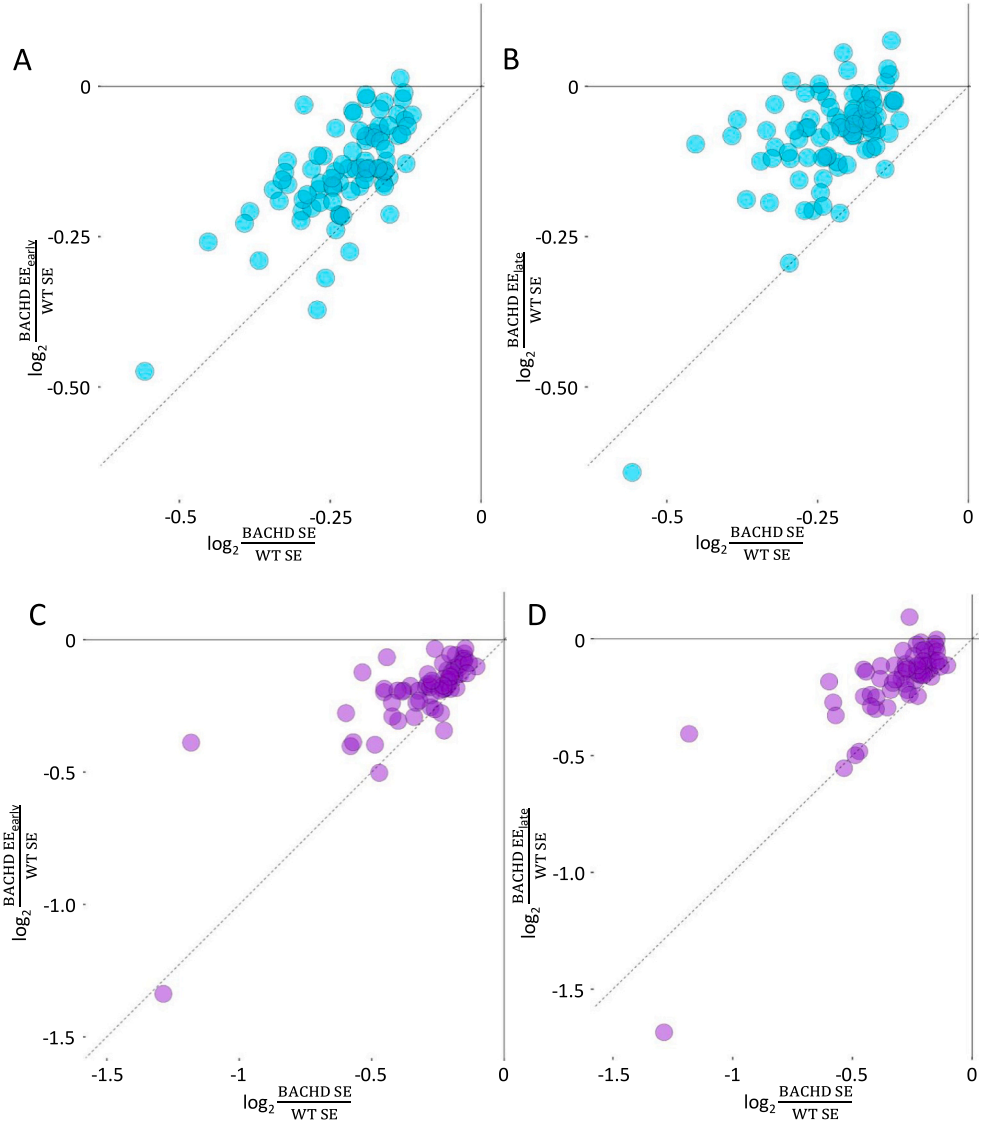

Fig. 6. Environmental enrichment normalized expression disturbances in transgenic animals.
Comparisons of $\log_2$ fold DEG expression changes between 12-month-old WT SE animals and transgenic rats: Relative module Cyan DEGs expression in BACHD SE vs. BACHD EE_{early} **(A)** and in BACHD SE vs. BACHD EE_{late} **(B)**. **(C)** and **(D)** show $\log_2$ fold changes in module Purple DEGs in BACHD SE vs. BACHD EE_{early} and BACHD SE vs. BACHD EE_{late}, respectively. The dotted line represents the ordinary diagonal that signifies identical relative expression changes in both conditions. N values were 7 (WT SE), 6 (WT EE_{early}), 6 (WT EE_{late}), 6 (BACHD SE), 6 (BACHD EE_{early}), 6 (BACHD EE_{late}), respectively. (For interpretation of the references to colour in this figure legend, the reader is referred to the web version of this article.)

(*difference* = 11.6; critical difference for $\alpha_{adjusted}$ = 0.05 was 26.9 and 23.7 for module Cyan and Purple, respectively).

These findings show that environmental enrichment could normalize expression disturbances in transgenic animals. Regarding module Cyan genes, the EE_{late} group displayed an even greater ameliorative effect, highlighting the potential of timed interventions and the need to diversify study designs implementing environmental enrichment.

4. Discussion

This study examined the behavioural and striatal transcriptome disturbances in a transgenic rat model overexpressing mHTT and the potential of two designs of environmental stimuli to modify such disturbances. Gene network analyses indicated co-expression clusters preserved in rodents and human expression data with widespread dysregulation of gene activity under standard conditions. Altered expression of genes related to myelination and synaptic function is in agreement with recent HD research (Barron et al., 2021; Cepeda and Levine, 2022; Raymond, 2017; Smith-Dijak et al., 2019; Bourbon-Teles et al., 2019; Ferrari Bardile et al., 2019; Casella et al., 2020). Examining age-related module changes, trajectories were in general comparable between both genotypes. Yet, BACHD animals displayed a partial failure to reach or maintain expression levels shown by their WT counterparts. Intriguingly, environmental enrichment moderated mHTT-induced transcriptional disturbances both at early and later exposure with a tendency for the latter to show even greater effect. Similarly, behavioural data indicated a marked transgene-induced effect on weight, cognitive performance, anxiety-related behaviour and locomotor activity with the older cohorts showing worse phenotypic changes and minor influence from environmental enrichment. Importantly, mediating effects on performance in individual domains need to be considered when interpreting behavioural test results. For example, poorer performance of BACHD animals in both age cohorts may not only be explained by impaired cognitive functioning, but also mobility deficits as PhenoMaster data show reduced locomotor activity in transgenic animals. Since no genotype-related effects were observed during the acquisition phase of the experiment in either age cohort, motoric symptoms did not seem to have greatly influenced the performance of BACHD animals, further indicating mHTT-induced effects on non-motor domains.

This study only examined female animals in accordance with the local Animal Welfare and Ethics committee, as aggressive behaviour has been reported to occur between male animals housed in a long-term enriched environment (Marashi et al., 2003). However, sex differences in responses to EE have been observed, especially regarding cognitive domains (Wood et al., 2010; Winberg et al., 2022). This underlines the importance of considering potential sexual dimorphism in future EE protocols.

Within the identified modules, several genes may act as modifiers of HD pathology. One example is the myelin basic protein *Mbp* gene, which was expressed within module Cyan and displayed mHTT-induced dysregulation. Previous research has linked decreased *Mbp* expression with a thinning of myelin sheaths prior to the onset of behavioural symptoms of HD (Xiang et al., 2011). The Myelin Associated Glycoprotein (MAG), encoded by the *Mag* gene and included in module Cyan, accounts for less than 1 % of myelin sheath proteins of both the central and peripheral nervous system (Trapp, 1990), yet MAG is vital for axon-myelin interaction and stability (Quarles, 2007; Kinter et al., 2013). In animal studies of MAG-deficient mice, both myelin and axonal degeneration was observed (Fruttiger et al., 1995; Yin et al., 1998; Pan et al., 2005), with similar findings being reported for patients with loss of function mutations in *MAG (*Lossos et al., *2015)*. Further, module Purple included genes like *Cryab* that encodes the heat shock protein αB-crystallin. αB-crystallin effectively antagonizes protein aggregation and has been found as a neuroprotective agent in animal models of Parkinson's disease, amyotrophic lateral sclerosis, Alzheimer's disease, as well as Huntington's disease (Tue et al., 2012; Hagemann et al., 2009; Wang et al., 2005; Waudby et al., 2010; Hochberg et al., 2014). In a study on BACHD mice, αB-crystallin levels decreased over time and astrocytic Cryab overexpression led to an improved phenotype (Oliveira et al., 2016). As a regulator of mitochondrial and endosomal fission, Dynamin 2 (*Dnm2*) plays a pivotal role in cellular energy management and autophagy (Puri et al., 2020; Kraus and Ryan, 2017), both of which are impaired in HD (Jurcau, 2022). Additionally, DNM2 is a primary HTT-interacting protein (Tourette et al., 2014) and known to cause or modify a range of neuromuscular diseases (Zhao et al., 2018).

The present study aimed to advance our understanding of how genetic endowment and environmental factors interact transcriptiobally to shape baviour. We found clear evidence for the concept of an "*environmental rescue*" on transcriptome level, where transgenic dysregulation could successfully be prevented by different types of environmental enrichment. We identified candidate genes that may mediate this protective effect and represent targets for further research. Our findings highlight the promising potential of enviromimetics and encourage to further advance our understanding of the complex interactions between genetic and environmental factors in the pathogenesis and clinical management of Chorea Huntington and other neuropsychiatric diseases.

Interestingly, this study showed that environmental enrichment both at early and later age was able to normalize expression levels of these candidate genes as well as their co-expressed dysregulated module genes, making them interesting candidates as mediators of the environmental influence on HD pathology. This highlights the potential of HD-modifying lifestyle interventions and provides evidence that HD patients can benefit from an active and enriched lifestyle even later at age and after disease onset.

CRediT authorship contribution statement

A. Kilzheimer: Writing – original draft, Visualization, Methodology, Investigation, Formal analysis, Data analyis and curation. **T. Hentrich:** Writing – review & editing, Visualization, Software, Methodology, Formal analysis, Data curation. **A. Novati:** Validation, Investigation, Formal analysis. **H. Nguyen:** Designed the experiments and gave guidance for the BACH model. **Z. Wassouf:** Writing – review & editing, Validation, Investigation, Formal analysis, Conceptualization. **J.M. Schulze-Hentrich:** Writing – review & editing, Supervision, Project administration, Formal analysis, Conceptualization.

Funding

This work was supported by an IZKF junior group fund from the Medical Faculty of University Tübingen. AK was supported by a scholarship from the IZKF-Promotionskolleg Tübingen. The NGS Competence Center Tübingen received funding through the DFG (NCCT-DFG, project 407494995).

Declaration of competing interest

The authors declare that they have no known competing financial interests or personal relationships that could have appeared to influence the work reported in this paper.

Acknowledgements

We thank Elisabeth Gustafsson, Ilona Los and Celina Tomczak for her animal work assistance and Olaf Riess for advice and discussions. In addition, we would like to thank the core facility NCCT for preparing the libraries and sequencing the samples.

Appendix A. Supplementary data

Supplementary data to this article can be found online at https://doi.org/10.1016/j.expneurol.2025.115561.

Data availability

RNA-seq data files have been uploaded to GEO database and are available under the accession number [pending submission validation].

References

Barron, J.C., Hurley, E.P., Parsons, M.P., 2021. Huntingtin and the synapse. Front. Cell. Neurosci. 15, 689332.

Bates, G.P., 2005. History of genetic disease: the molecular genetics of Huntington disease - a history. Nat. Rev. Genet. 6 (10), 766–773.

Benn, C.L., Luthi-Carter, R., Kuhn, A., Sadri-Vakili, G., Blankson, K.L., Dalai, S.C., et al., 2010. Environmental enrichment reduces neuronal intranuclear inclusion load but has no effect on messenger RNA expression in a mouse model of Huntington disease. J. Neuropathol. Exp. Neurol. 69 (8), 817–827.

Boggs, J.M., 2006. Myelin basic protein: a multifunctional protein. Cell. Mol. Life Sci. 63 (17), 1945–1961.

Bourbon-Teles, J., Bells, S., Jones, D.K., Coulthard, E., Rosser, A., Metzler-Baddeley, C., 2019. Myelin breakdown in human Huntington's disease: multi-modal evidence from diffusion MRI and quantitative magnetization transfer. Neuroscience 403, 79–92.

Casella, C., Lipp, I., Rosser, A., Jones, D.K., Metzler-Baddeley, C., 2020. A critical review of white matter changes in Huntington's disease. Mov. Disord. 35 (8), 1302–1311.

Cepeda, C., Levine, M.S., 2022. Synaptic dysfunction in Huntington's disease: lessons from genetic animal models. Neuroscientist 28 (1), 20–40.

Cha, J.H., 2007. Transcriptional signatures in Huntington's disease. Prog. Neurobiol. 83 (4), 228–248.

Couly, S., Carles, A., Denus, M., Benigno-Anton, L., Maschat, F., Maurice, T., 2021. Exposure of R6/2 mice in an enriched environment augments P42 therapy efficacy on Huntington's disease progression. Neuropharmacology 186, 108467.

Curtin, P.C., Farrar, A.M., Oakeshott, S., Sutphen, J., Berger, J., Mazzella, M., et al., 2015. Cognitive training at a young age attenuates deficits in the zQ175 mouse model of HD. Front. Behav. Neurosci. 9, 361.

DiFiglia, M., Sapp, E., Chase, K.O., Davies, S.W., Bates, G.P., Vonsattel, J.P., Aronin, N., 1997. Aggregation of huntingtin in neuronal intranuclear inclusions and dystrophic neurites in brain. Science 277 (5334), 1990-3.

Dobin, A., Davis, C.A., Schlesinger, F., Drenkow, J., Zaleski, C., Jha, S., et al., 2013. STAR: ultrafast universal RNA-seq aligner. Bioinformatics 29 (1), 15–21.

Du, X., Leang, L., Mustafa, T., Renoir, T., Pang, T.Y., Hannan, A.J., 2012. Environmental enrichment rescues female-specific hyperactivity of the hypothalamic-pituitary-adrenal axis in a model of Huntington's disease. Transl. Psychiatry 2 (7), e133.

Dubois, C., Kong, G., Tran, H., Li, S., Pang, T.Y., Hannan, A.J., Renoir, T., 2021. Small non-coding RNAs are dysregulated in Huntington's disease transgenic mice independently of the therapeutic effects of an environmental intervention. Mol. Neurobiol. 58 (7), 3308–3318.

Durrenberger, P.F., Fernando, F.S., Kashefi, S.N., Bonnert, T.P., Seilhean, D., Nait-Oumesmar, B., et al., 2015. Common mechanisms in neurodegeneration and neuroinflammation: a BrainNet Europe gene expression microarray study. J. Neural Transm. (Vienna) 122 (7), 1055–1068.

Ehrlich, M.E., 2012. Huntington's disease and the striatal medium spiny neuron: cell-autonomous and non-cell-autonomous mechanisms of disease. Neurotherapeutics 9 (2), 270–284.

Ferrari Bardile, C., Garcia-Miralles, M., Caron, N.S., Rayan, N.A., Langley, S.R., Harmston, N., et al., 2019. Intrinsic mutant HTT-mediated defects in oligodendroglia cause myelination deficits and behavioral abnormalities in Huntington disease. Proc. Natl. Acad. Sci. U. S. A. 116 (19), 9622–9627.

Fruttiger, M., Montag, D., Schachner, M., Martini, R., 1995. Crucial role for the myelin-associated glycoprotein in the maintenance of axon-myelin integrity. Eur. J. Neurosci. 7 (3), 511–515.

Glass, M., van Dellen, A., Blakemore, C., Hannan, A.J., Faull, R.L., 2004. Delayed onset of Huntington's disease in mice in an enriched environment correlates with delayed loss of cannabinoid CB1 receptors. Neuroscience 123 (1), 207–212.

Gubert, C., Love, C.J., Kodikara, S., Mei Liew, J.J., Renoir, T., Le Cao, K.A., Hannan, A.J., 2022. Gene-environment-gut interactions in Huntington's disease mice are associated with environmental modulation of the gut microbiome. iScience 25 (1), 103687.

Gusella, J.F., MacDonald, M.E., Lee, J.M., 2014. Genetic modifiers of Huntington's disease. Mov. Disord. 29 (11), 1359–1365.

Hagemann, T.L., Boelens, W.C., Wawrousek, E.F., Messing, A., 2009. Suppression of GFAP toxicity by alphaB-crystallin in mouse models of Alexander disease. Hum. Mol. Genet. 18 (7), 1190–1199.

Halliday, G.M., McRitchie, D.A., Macdonald, V., Double, K.L., Trent, R.J., McCusker, E., 1998. Regional specificity of brain atrophy in Huntington's disease. Exp. Neurol. 154 (2), 663–672.

Hochberg, G.K., Ecroyd, H., Liu, C., Cox, D., Cascio, D., Sawaya, M.R., et al., 2014. The structured core domain of alphaB-crystallin can prevent amyloid fibrillation and associated toxicity. Proc. Natl. Acad. Sci. U. S. A. 111 (16), E1562–E1570.

Hockly, E., Cordery, P.M., Woodman, B., Mahal, A., van Dellen, A., Blakemore, C., et al., 2002. Environmental enrichment slows disease progression in R6/2 Huntington's disease mice. Ann. Neurol. 51 (2), 235–242.

Hodges, A., Strand, A.D., Aragaki, A.K., Kuhn, A., Sengstag, T., Hughes, G., et al., 2006. Regional and cellular gene expression changes in human Huntington's disease brain. Hum. Mol. Genet. 15 (6), 965–977.

Jurcau, A., 2022. Molecular pathophysiological mechanisms in Huntington's disease. Biomedicines 10 (6).

Keum, J.W., Shin, A., Gillis, T., Mysore, J.S., Abu Elneel, K., Lucente, D., et al., 2016. The HTT CAG-expansion mutation determines age at death but not disease duration in Huntington disease. Am. J. Hum. Genet. 98 (2), 287–298.

Kim, A., Lalonde, K., Truesdell, A., Gomes Welter, P., Brocardo, P.S., Rosenstock, T.R., Gil-Mohapel, J., 2021. New avenues for the treatment of Huntington's disease. Int. J. Mol. Sci. 22 (16).

Kinter, J., Lazzati, T., Schmid, D., Zeis, T., Erne, B., Lutzelschwab, R., et al., 2013. An essential role of MAG in mediating axon-myelin attachment in Charcot-Marie-Tooth 1A disease. Neurobiol. Dis. 49, 221–231.

Kraus, F., Ryan, M.T., 2017. The constriction and scission machineries involved in mitochondrial fission. J. Cell Sci. 130 (18), 2953–2960.

Kreilaus, F., Spiro, A.S., Hannan, A.J., Garner, B., Jenner, A.M., 2016. Therapeutic effects of anthocyanins and environmental enrichment in R6/1 Huntington's disease mice. J. Huntingtons Dis. 5 (3), 285–296.

Kumar, A., Vaish, M., Ratan, R.R., 2014. Transcriptional dysregulation in Huntington's disease: a failure of adaptive transcriptional homeostasis. Drug Discov. Today 19 (7), 956–962.

Langfelder, P., Horvath, S., 2008. WGCNA: an R package for weighted correlation network analysis. BMC Bioinform. 9, 559.

Langfelder, P., Horvath, S., 2012. Fast R Functions for Robust Correlations and Hierarchical Clustering. J Stat Softw 46 (11).

Langfelder, P., Cantle, J.P., Chatzopoulou, D., Wang, N., Gao, F., Al-Ramahi, I., et al., 2016. Integrated genomics and proteomics define huntingtin CAG length-dependent networks in mice. Nat. Neurosci. 19 (4), 623–633.

Lazic, S.E., Grote, H.E., Blakemore, C., Hannan, A.J., van Dellen, A., Phillips, W., Barker, R.A., 2006. Neurogenesis in the R6/1 transgenic mouse model of Huntington's disease: effects of environmental enrichment. Eur. J. Neurosci. 23 (7), 1829–1838.

Li, H., Handsaker, B., Wysoker, A., Fennell, T., Ruan, J., Homer, N., et al., 2009. The sequence alignment/map format and SAMtools. Bioinformatics 25 (16), 2078–2079.

Lossos, A., Elazar, N., Lerer, I., Schueler-Furman, O., Fellig, Y., Glick, B., et al., 2015. Myelin-associated glycoprotein gene mutation causes Pelizaeus-Merzbacher disease-like disorder. Brain 138 (Pt 9), 2521–2536.

Love, M.I., Huber, W., Anders, S., 2014. Moderated estimation of fold change and dispersion for RNA-seq data with DESeq2. Genome Biol. 15 (12), 550.

Lu, S.Z., Guo, Y.S., Liang, P.Z., Zhang, S.Z., Yin, S., Yin, Y.Q., et al., 2019. Suppression of astrocytic autophagy by alphaB-crystallin contributes to alpha-synuclein inclusion formation. Transl. Neurodegener. 8, 3.

Mantovani, S., Gordon, R., Li, R., Christie, D.C., Kumar, V., Woodruff, T.M., 2016. Motor deficits associated with Huntington's disease occur in the absence of striatal degeneration in BACHD transgenic mice. Hum. Mol. Genet. 25 (9), 1780–1791.

Marashi, V., Barnekow, A., Ossendorf, E., Sachser, N., 2003. Effects of different forms of environmental enrichment on behavioral, endocrinological, and immunological parameters in male mice. Horm. Behav. 43 (2), 281–292.

Marder, K., Zhao, H., Eberly, S., Tanner, C.M., Oakes, D., Shoulson, I., Huntington Study G, 2009. Dietary intake in adults at risk for Huntington disease: analysis of PHAROS research participants. Neurology 73 (5), 385–392.

Mazarakis, N.K., Mo, C., Renoir, T., van Dellen, A., Deacon, R., Blakemore, C., Hannan, A.J., 2014. Super-enrichment' reveals dose-dependent therapeutic effects of environmental stimulation in a transgenic mouse model of Huntington's disease. J. Huntingtons Dis. 3 (3), 299–309.

McColgan, P., Tabrizi, S.J., 2018. Huntington's disease: a clinical review. Eur. J. Neurol. 25 (1), 24–34.

Mees, I., Li, S., Tran, H., Ang, C.S., Williamson, N.A., Hannan, A.J., Renoir, T., 2022. Phosphoproteomic dysregulation in Huntington's disease mice is rescued by environmental enrichment. Brain Commun. 4 (6), fcac305.

Menalled, L., El-Khodor, B.F., Patry, M., Suarez-Farinas, M., Orenstein, S.J., Zahasky, B., et al., 2009. Systematic behavioral evaluation of Huntington's disease transgenic and knock-in mouse models. Neurobiol. Dis. 35 (3), 319–336.

Mo, C., Renoir, T., Pang, T.Y., Hannan, A.J., 2013. Short-term memory acquisition in female Huntington's disease mice is vulnerable to acute stress. Behav. Brain Res. 253, 318–322.

Mo, C., Hannan, A.J., Renoir, T., 2015. Environmental factors as modulators of neurodegeneration: insights from gene-environment interactions in Huntington's disease. Neurosci. Biobehav. Rev. 52, 178–192.

Nithianantharajah, J., Barkus, C., Murphy, M., Hannan, A.J., 2008. Gene-environment interactions modulating cognitive function and molecular correlates of synaptic plasticity in Huntington's disease transgenic mice. Neurobiol. Dis. 29 (3), 490–504.

Novati, A., Hentrich, T., Wassouf, Z., Weber, J.J., Yu-Taeger, L., Deglon, N., et al., 2018. Environment-dependent striatal gene expression in the BACHD rat model for Huntington disease. Sci. Rep. 8 (1), 5803.

Novati, A., Nguyen, H.P., Schulze-Hentrich, J., 2022. Environmental stimulation in Huntington disease patients and animal models. Neurobiol. Dis. 171, 105725.

Oliveira, A.O., Osmand, A., Outeiro, T.F., Muchowski, P.J., Finkbeiner, S., 2016. alphaB-Crystallin overexpression in astrocytes modulates the phenotype of the BACHD mouse model of Huntington's disease. Hum. Mol. Genet. 25 (9), 1677–1689.

Pan, B., Fromholt, S.E., Hess, E.J., Crawford, T.O., Griffin, J.W., Sheikh, K.A., Schnaar, R. L., 2005. Myelin-associated glycoprotein and complementary axonal ligands, gangliosides, mediate axon stability in the CNS and PNS: neuropathology and behavioral deficits in single- and double-null mice. Exp. Neurol. 195 (1), 208–217.

Pang, T.Y., Du, X., Zajac, M.S., Howard, M.L., Hannan, A.J., 2009. Altered serotonin receptor expression is associated with depression-related behavior in the R6/1 transgenic mouse model of Huntington's disease. Hum. Mol. Genet. 18 (4), 753–766.

Papoutsi, M., Labuschagne, I., Tabrizi, S.J., Stout, J.C., 2014. The cognitive burden in Huntington's disease: pathology, phenotype, and mechanisms of compensation. Mov. Disord. 29 (5), 673–683.
Puri, C., Manni, M.M., Vicinanza, M., Hilcenko, C., Zhu, Y., Runwal, G., et al., 2020. A DNM2 centronuclear myopathy mutation reveals a link between recycling endosome scission and autophagy. Dev. Cell 53 (2), 154–68 e6.
Quarles, R.H., 2007. Myelin-associated glycoprotein (MAG): past, present and beyond. J. Neurochem. 100 (6), 1431–1448.
Raasakka, A., Ruskamo, S., Kowal, J., Barker, R., Baumann, A., Martel, A., et al., 2017. Membrane association landscape of Myelin basic protein portrays formation of the Myelin major dense line. Sci. Rep. 7 (1), 4974.
Raymond, L.A., 2017. Striatal synaptic dysfunction and altered calcium regulation in Huntington disease. Biochem. Biophys. Res. Commun. 483 (4), 1051–1062.
Renoir, T., Pang, T.Y., Mo, C., Chan, G., Chevarin, C., Lanfumey, L., Hannan, A.J., 2013. Differential effects of early environmental enrichment on emotionality related behaviours in Huntington's disease transgenic mice. J. Physiol. 591 (1), 41–55.
Rub, U., Seidel, K., Heinsen, H., Vonsattel, J.P., den Dunnen, W.F., Korf, H.W., 2016. Huntington's disease (HD): the neuropathology of a multisystem neurodegenerative disorder of the human brain. Brain Pathol. 26 (6), 726–740.
Schilling, G., Savonenko, A.V., Coonfield, M.L., Morton, J.L., Vorovich, E., Gale, A., et al., 2004. Environmental, pharmacological, and genetic modulation of the HD phenotype in transgenic mice. Exp. Neurol. 187 (1), 137–149.
Simonin, C., Duru, C., Salleron, J., Hincker, P., Charles, P., Delval, A., et al., 2013. Association between caffeine intake and age at onset in Huntington's disease. Neurobiol. Dis. 58, 179–182.
Skillings, E.A., Wood, N.I., Morton, A.J., 2014. Beneficial effects of environmental enrichment and food entrainment in the R6/2 mouse model of Huntington's disease. Brain Behav. 4 (5), 675–686.
Smith-Dijak, A.I., Sepers, M.D., Raymond, L.A., 2019. Alterations in synaptic function and plasticity in Huntington disease. J. Neurochem. 150 (4), 346–365.
Spires, T.L., Grote, H.E., Varshney, N.K., Cordery, P.M., van Dellen, A., Blakemore, C., Hannan, A.J., 2004. Environmental enrichment rescues protein deficits in a mouse model of Huntington's disease, indicating a possible disease mechanism. J. Neurosci. 24 (9), 2270–2276.
Steventon, J.J., Harrison, D.J., Trueman, R.C., Rosser, A.E., Jones, D.K., Brooks, S.P., 2015. In vivo MRI evidence that neuropathology is attenuated by cognitive enrichment in the Yac128 Huntington's disease mouse model. J. Huntingtons Dis. 4 (2), 149–160.
Tabrizi, S.J., Langbehn, D.R., Leavitt, B.R., Roos, R.A., Durr, A., Craufurd, D., et al., 2009. Biological and clinical manifestations of Huntington's disease in the longitudinal TRACK-HD study: cross-sectional analysis of baseline data. Lancet Neurol. 8 (9), 791–801.
Tabrizi, S.J., Scahill, R.I., Owen, G., Durr, A., Leavitt, B.R., Roos, R.A., et al., 2013. Predictors of phenotypic progression and disease onset in premanifest and early-stage Huntington's disease in the TRACK-HD study: analysis of 36-month observational data. Lancet Neurol. 12 (7), 637–649.
Thorvaldsdottir, H., Robinson, J.T., Mesirov, J.P., 2013. Integrative Genomics Viewer (IGV): high-performance genomics data visualization and exploration. Brief. Bioinform. 14 (2), 178–192.
Tourette, C., Li, B., Bell, R., O'Hare, S., Kaltenbach, L.S., Mooney, S.D., Hughes, R.E., 2014. A large scale Huntingtin protein interaction network implicates Rho GTPase signaling pathways in Huntington disease. J. Biol. Chem. 289 (10), 6709–6726.
Trapp, B.D., 1990. Myelin-associated glycoprotein. Location and potential functions. Ann. N. Y. Acad. Sci. 605, 29–43.
Trembath, M.K., Horton, Z.A., Tippett, L., Hogg, V., Collins, V.R., Churchyard, A., et al., 2010. A retrospective study of the impact of lifestyle on age at onset of Huntington disease. Mov. Disord. 25 (10), 1444–1450.
Trovato, B., Magri, B., Castorina, A., Maugeri, G., D'Agata, V., Musumeci, G., 2022. Effects of exercise on skeletal muscle pathophysiology in Huntington's disease. J. Funct. Morphol. Kinesiol. 7 (2).
Tue, N.T., Shimaji, K., Tanaka, N., Yamaguchi, M., 2012. Effect of alphaB-crystallin on protein aggregation in Drosophila. J. Biomed. Biotechnol. 2012, 252049.
van Dellen, A., Blakemore, C., Deacon, R., York, D., Hannan, A.J., 2000. Delaying the onset of Huntington's in mice. Nature 404 (6779), 721–722.
van Duijn, E., Craufurd, D., Hubers, A.A., Giltay, E.J., Bonelli, R., Rickards, H., et al., 2014. Neuropsychiatric symptoms in a European Huntington's disease cohort (REGISTRY). J. Neurol. Neurosurg. Psychiatry 85 (12), 1411–1418.
Waldvogel, H.J., Kim, E.H., Tippett, L.J., Vonsattel, J.P., Faull, R.L., 2015. The neuropathology of Huntington's disease. Curr. Top. Behav. Neurosci. 22, 33–80.
Wang, J., Xu, G., Li, H., Gonzales, V., Fromholt, D., Karch, C., et al., 2005. Somatodendritic accumulation of misfolded SOD1-L126Z in motor neurons mediates degeneration: alphaB-crystallin modulates aggregation. Hum. Mol. Genet. 14 (16), 2335–2347.
Waudby, C.A., Knowles, T.P., Devlin, G.L., Skepper, J.N., Ecroyd, H., Carver, J.A., et al., 2010. The interaction of alphaB-crystallin with mature alpha-synuclein amyloid fibrils inhibits their elongation. Biophys. J. 98 (5), 843–851.
Wetzels, R., Wagenmakers, E.J., 2012. A default Bayesian hypothesis test for correlations and partial correlations. Psychon. Bull. Rev. 19 (6), 1057–1064.
Winberg, J., Rentz, J., Sugamori, K., Swardfager, W., Mitchell, J., 2022. Sex differences in metabolic and behavioral responses to exercise but not exogenous osteocalcin treatment in mice fed a high fat diet. Front. Physiol. 13, 831056.
Wood, N.I., Carta, V., Milde, S., Skillings, E.A., McAllister, C.J., Ang, Y.L., et al., 2010. Responses to environmental enrichment differ with sex and genotype in a transgenic mouse model of Huntington's disease. PloS One 5 (2), e9077.
Wood, N.I., Glynn, D., Morton, A.J., 2011. "Brain training" improves cognitive performance and survival in a transgenic mouse model of Huntington's disease. Neurobiol. Dis. 42 (3), 427–437.
Xiang, Z., Valenza, M., Cui, L., Leoni, V., Jeong, H.K., Brilli, E., et al., 2011. Peroxisome-proliferator-activated receptor gamma coactivator 1 alpha contributes to dysmyelination in experimental models of Huntington's disease. J. Neurosci. 31 (26), 9544–9553.
Yin, X., Crawford, T.O., Griffin, J.W., Tu, P., Lee, V.M., Li, C., et al., 1998. Myelin-associated glycoprotein is a myelin signal that modulates the caliber of myelinated axons. J. Neurosci. 18 (6), 1953–1962.
Yu-Taeger, L., Petrasch-Parwez, E., Osmand, A.P., Redensek, A., Metzger, S., Clemens, L. E., et al., 2012. A novel BACHD transgenic rat exhibits characteristic neuropathological features of Huntington disease. J. Neurosci. 32 (44), 15426–15438.
Zajac, M.S., Pang, T.Y., Wong, N., Weinrich, B., Leang, L.S., Craig, J.M., et al., 2010. Wheel running and environmental enrichment differentially modify exon-specific BDNF expression in the hippocampus of wild-type and pre-motor symptomatic male and female Huntington's disease mice. Hippocampus 20 (5), 621–636.
Zajac, M.S., Renoir, T., Perreau, V.M., Li, S., Adams, W., van den Buuse, M., Hannan, A. J., 2018. Short-term environmental stimulation spatiotemporally modulates specific serotonin receptor gene expression and behavioral pharmacology in a sexually dimorphic manner in Huntington's disease transgenic mice. Front. Mol. Neurosci. 11, 433.
Zaykin, D.V., 2011. Optimally weighted Z-test is a powerful method for combining probabilities in meta-analysis. J. Evol. Biol. 24 (8), 1836–1841.
Zhang, B., Horvath, S., 2005. A general framework for weighted gene co-expression network analysis. Stat. Appl. Genet. Mol. Biol. 4, 17.
Zhao, M., Maani, N., Dowling, J.J., 2018. Dynamin 2 (DNM2) as cause of, and modifier for, human neuromuscular disease. Neurotherapeutics 15 (4), 966–975.
Zhunina, O.A., Yabbarov, N.G., Orekhov, A.N., Deykin, A.V., 2019. Modern approaches for modelling dystonia and Huntington's disease in vitro and in vivo. Int. J. Exp. Pathol. 100 (2), 64–71.